PHYSICAL REVIEW D VOLUME 25 , NUMBER 11 1 JUNE 1982

Hadron-nucleus interactions at high energies

Charles B. Chiu
Center for Particle Theory, Department of Physics, University of Texas at Austin, Austin, Texas 78712

Zuoxiu He
Institute of Theoretical Physics, Academia Sinica, Beijing, People's Republic of China

Don M. Tow
*Center for Particle Theory, Department of Physics, University of Texas at Austin, Austin, Texas 78712 and Bell Telephone Laboratories, Holmdel, New Jersey 07733**

(Received 20 April 1981)

A simple space-time description of high-energy hadron-nucleus interactions is presented. The model is based on the DTU (dual topological unitarization) -parton-model description of soft multiparticle production in hadron-hadron interactions. The essentially parameter-free model agrees well with the general features of high-energy data for hadron-nucleus interactions; in particular, this DTU-parton model has a natural explanation for an approximate $\bar{\nu}$ universality. The extension to high-energy nucleus-nucleus interactions is presented. We also compare and contrast this model with several previously proposed models.

I. INTRODUCTION

In hadron-hadron (hh) scattering experiments, because the particle detectors are always at macroscopic distances from the interaction region,[1] one can never learn about the space-time development of the strongly interacting process. In other words, hh scattering experiments can only measure the S matrix. On the other hand, if one replaces the target hadron by a nuclear target, then the time of flight for the incident hadron or any produced secondary in traveling from the first nucleon to a succeeding nucleon in the nucleus is of the same order or even shorter than the typical duration of the strongly interacting process. This means the nucleons in the nucleus serve as detectors which are separated by microscopic distances. Therefore, hadron-nucleus (hA) scattering experiments offer the unique opportunity to learn about the space-time development of a strongly interacting process. Furthermore, one of the important areas of research in strong interactions during the past decade has been to find the correct model for describing high-energy multiparticle production processes. Since different multiparticle production models for hh collisions give rise in general to different predictions for hA collisions, studying hA interactions provides a good possibility of discriminating among the various multiparticle production models and selecting the correct one. For these reasons, high-energy hA collisions have generated tremendous interest during the past few years, both experimentally and theoretically.[2]

In this paper, we discuss a simple space-time description of high-energy hA interactions.[3] The model is motivated by recent developments in the dual topological unitarization (DTU) approach[4] to soft hadronic interaction; the latter approach has also been shown to be closely related to the parton model.[5,6] For brevity, we call this model the DTU-parton model or the two-sheet model. We will show that this simple model can explain many general features of the high-energy hA data.

We first review in Sec. II the essential features of the experimental hA multiparticle production data. Our theoretical model is presented in Sec. III, together with the comparison with data. The $\bar{\nu}$-universality feature is also discussed in this section. This is followed by Sec. IV on the extension to nucleus-nucleus (AA) interactions. Section V com-

pares and contrasts this model with several previously proposed models. Section VI contains a brief conclusion and mentions some other interesting effects arising from interactions with nuclear targets. In the Appendix we show how one can improve the quantitative calculations by estimating the next-order correction.

II. EXPERIMENTAL FEATURES

There are several general features of the data.[7] One defines

$$\bar{\nu}_h \equiv \frac{A\sigma_{\text{in}}^{hN}}{\sigma_{\text{in}}^{hA}} , \tag{2.1}$$

where σ_{in}^{hN} (σ_{in}^{hA}) is the hadron-nucleon (-nucleus) inelastic cross section and A is the number of nucleons in the nucleus. The variable $\bar{\nu}_h$ can be interpreted to be the average number of inelastic collisions experienced by the hadron h as it traverses the nucleus.[8] Experimentally $\bar{\nu}_h$ is approximately energy independent in the Fermilab energy range. Table I gives the values of $\bar{\nu}$ for p and $\pi^{\pm}$ from an experiment[7(b)] in the energy range from 50 to 200 GeV.

If one defines

$$R_A \equiv \frac{\langle N_{\text{ch}} \rangle_{hA}}{\langle N_{\text{ch}} \rangle_{hN}} , \tag{2.2}$$

then the first feature is as follows.

(a) R_A is small (~ 2.5) even for the largest A (see Fig. 1) and may be approximately parametrized as

$$R_A \cong a + b\bar{\nu}_h, \quad \text{with } a \cong \tfrac{1}{2} \cong b \tag{2.3}$$

TABLE I. Values of $\bar{\nu}$ for p and $\pi^{\pm}$ from an experiment [Ref. 7(b)] in the energy range from 50 to 200 GeV.

Element	A	$\bar{\nu}_p$	$\bar{\nu}_\pi$
H	1	1.00	1.00
C	12	1.52	1.39
Al	27	1.95	1.70
emulsion	~ 60	2.50	2.07
Cu	64	2.54	2.10
Ag	108	3.00	2.40
Pb	207	3.67	2.82
U	238	3.84	2.92

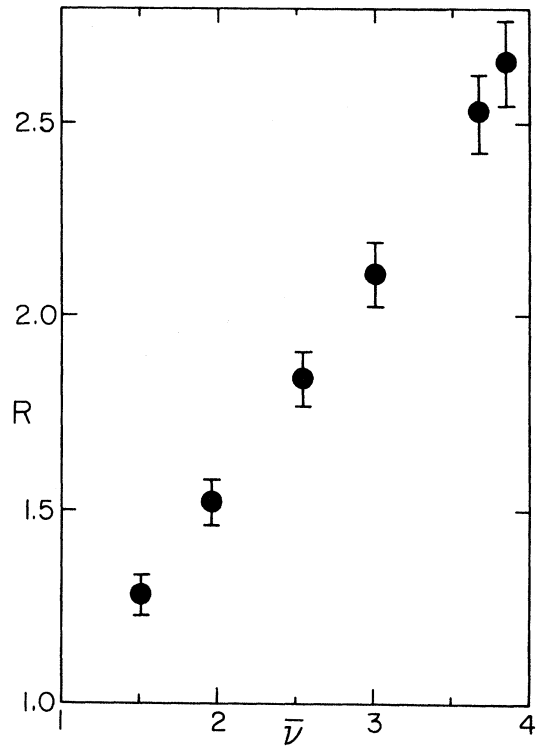

FIG. 1. The multiplicity ratio R_A versus $\bar{\nu}_p$ for 200-GeV pA collisions. Data are from Ref. 2(d).

where a and b are roughly energy independent in the Fermilab range.[9]

Let η and y be the pseudorapidity and rapidity variable, respectively, defined as $\eta \equiv -\ln\tan(\theta_L/2)$ and $y = \frac{1}{2}\ln[(E+P_z)/(E-P_z)]$, where θ_L is the laboratory scattering angle and E and P_z are the laboratory energy and longitudinal momentum of the particle. Experimentally it is easier to measure η, whereas theoretically it is more convenient to use y. For almost all practical purposes, they can be used interchangeably. In any case one can always change from one to another by a simple kinematical transformation. The second feature is as follows.

(b) The differential multiplicity distribution $dN/d\eta$ is approximately target independent in the projectile fragmentation region and increases roughly as $\bar{\nu}_h$ in the target fragmentation region, as shown in Fig. 2.

Different projectiles give rise to different $\bar{\nu}_h$ and result in different R_A and $dN/d\eta$ for the same A. However, if we choose A such that we have the same $\bar{\nu}$ for different projectiles, then the third feature is as follows.

(c) Different projectiles but for the same $\bar{\nu}$ have

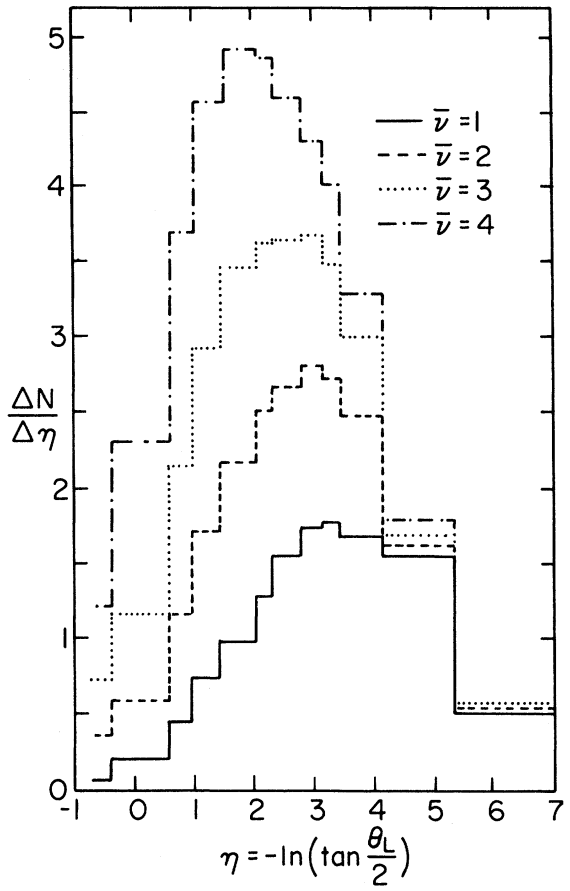

FIG. 2. Laboratory pseudorapidity distributions $dN/d\eta$ for pA collisions. Data are from Ref. 2(d).

almost the same R_A [Refs. 7(f) and 7(h)] and $dN/d\eta$.[7(b)] This feature is known as $\bar{\nu}$ universality.

As usual, one defines the elasticity to be the ratio of the laboratory energy of the outgoing projectile to the incident projectile's laboratory energy. For proton- or neutron-initiated reactions, there is little ambiguity in picking among the final hadrons the one corresponding to the projectile nucleon, because usually there is only one nucleon in the forward hemisphere. The fourth experimental feature is as follows.

(d) The elasticity for hA collisions decreases only slightly from that of hN collisions even for the largest A.[10]

Another feature is as follows.

(e) In the very forward region, i.e., for $\eta \sim \eta_{\max}$, $(dN/d\eta)^{hA_2} < (dN/d\eta)^{hA_1}$ by a small amount for $A_2 > A_1$.[7(e)]

Finally, if one defines

$$D \equiv (\langle N_{\rm ch}^2 \rangle - \langle N_{\rm ch} \rangle^2)^{1/2} , \tag{2.4}$$

the following is true.

(f) One sees a linear dependence of the dispersion D on $\langle N_{\rm ch} \rangle$, and the data points for various nuclei lie on the same straight line.[7(a)]

The above are six general features of the high-energy hA data. A successful model must explain most and eventually all of these features.

III. THE DTU-PARTON MODEL

We start with p-initiated reactions. Before considering the nuclear effects, we first consider the pN interaction. Within the DTU framework, at high energy the dominant contribution is that of the Pomeron which is described by the cylinder diagram of Fig. 3(a); cutting this diagram gives rise to the two-sheet diagram of Fig. 3(b), which describes the multiparticle production process a long time after the interaction. The basic underlying assumption of the model[3] is that shortly after the interaction the process is described by the same diagram, Fig. 3(b), but without the extra $q\bar{q}$ (quark-antiquark) pairs. This results in two hadronic systems: One consists of a projectile diquark and a target quark (we call this the excited projectile system EPS), and the other one consists of a target diquark and a projectile quark (we call this the excited target system ETS). Because of the large momentum difference between the diquark and the quark within each hadronic system, as time evolves the two colored ends of each hadronic system will be spatially separated and then the color-confining mechanism causes the hadronic systems to hadronize and so the above diagram evolves into the full diagram of Fig. 3(b).

We now discuss in more detail the above hadronization process and its application to pA interactions. Consider a hadronic system or sheet

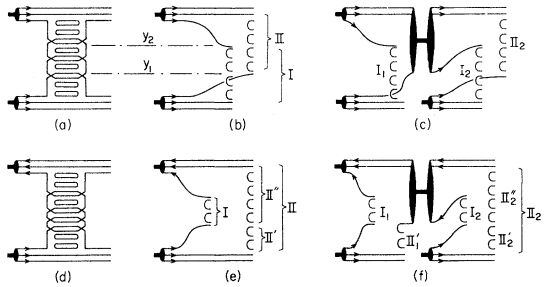

FIG. 3. Proton-initiated reactions: (a) Pomeron, (b) multiparticle production, (c) pA with $\bar{\nu}=2$. Antiproton-initiated reactions: (d) Pomeron, (e) multiparticle production, (f) $\bar{p}A$ with $\bar{\nu}=2$.

which is bounded by a colored object at each end and with the separation between these two colored objects increasing with time. The hadronization of this sytem means the production of $q\bar{q}$ pairs which then neutralize the color separation and result in a multihadron final state. A popular scheme for the confinement mechanism is to assume that the two colored objects form a one-dimensional chromoelectric flux tube which is analogous to the QED problem of an infinite parallel-plate capacitor with constant electric field. Then the production of a $q\bar{q}$ pair corresponds to the q and $\bar{q}$ penetrating a potential barrier.[11,12] This then leads in the rest frame of the pair to a universal (independent of the overall momentum of the pair) time τ_0 to produce this $q\bar{q}$ pair.[11–13] Transforming to the laboratory frame, this time is lengthened by a Lorentz-dilation factor $\gamma \cong \cosh y$, where y is the rapidity of the pair (since the pair has small relative momentum, y is also approximately the rapidity of q or $\bar{q}$). Now the time t that an object with rapidity y takes to travel the internucleon distance $d \cong 1/m_\pi$ is $t = d/\tanh y$. This leads to a critical rapidity $y_c \cong \sinh^{-1}(d/\tau_0)$, above which the $q\bar{q}$ pair will not have time to be produced. Strictly speaking, without solving the confinement problem, one does not know how to calculate τ_0 or y_c. Later on, we shall give some plausible arguments for their values.

We first present a description of our model which, although it is overly simplified, does allow one to quickly grasp the essence of the model. The EPS, being very energetic and so having a large Lorentz-dilation factor, does not have enough time to evolve into its asymptotic multiparticle final state upon reaching the next nucleon in A. On the other hand, the low-energy ETS, having a small Lorentz-dilation factor, has time to evolve into its asymptotic multiparticle final state upon reaching the next nucleon in A. The energies of the hadron from the evolution of the low-energy ETS are small and their further cascades in the first approximation can be neglected. This means for an interaction of hadron h with a nucleus characterized by a value of $\bar{\nu}_h$, there will be one EPS and $\bar{\nu}_h$ ETS's. This immediately leads to the experimental features (a) and (b).

We now present a more refined description which can be used for pA, as well as $\bar{p}A$ and πA, interactions. First we discuss what DTU tells us about the boundaries of the two sheets.[5,14] The double inclusive cross section for having a quark with rapidity y_1 and another with rapidity y_2 [see Fig. 3(b)] is

$$\frac{d\sigma}{dy_1 dy_2} \propto \exp[\alpha(Y-y_2)+\alpha_P(y_2-y_1)+\alpha y_1] , \tag{3.1}$$

where Y is the maximum laboratory rapidity, α and α_P are, respectively, the Reggeon and Pomeron intercepts. Using the relation

$$x_1 \cong -\exp\left[\left(\frac{Y}{2}-y_1\right)-\frac{Y}{2}\right] ,$$

$$x_2 \cong \exp\left[\left(y_2-\frac{Y}{2}\right)-\frac{Y}{2}\right] ,$$

we can rewrite (3.1) as

$$\frac{d\sigma}{dx_1 dx_2} \propto (-x_1 x_2)^{\alpha_P-\alpha-1} \cong (-x_1 x_2)^{-1/2} , \tag{3.2}$$

where the usual values of $\alpha \simeq \frac{1}{2}$ and $\alpha_P \simeq 1$ were used. This result says that the DTU dynamics, as given by the topology of Fig. 3(b), favors both quarks having a small $|x|$ value. Equation (3.2) says that for the present case, the boundaries of the two sheets are approximately given by the momentum distribution of the quark structure function. We emphasize that Eq. (3.2) is a result of DTU dynamics and its approximate agreement with the quark structure function here may be fortuitous. For the $\bar{\nu}$ universality to be valid, we shall see later that $y_c \geq y_1$ is required. In the following we shall first consider in detail the case $y_c \sim y_1$, and then discuss the inequality case. From Eq. (3.1), the first moment average values are $\langle y_1 \rangle = \langle Y-y_2 \rangle \simeq (\alpha_P-\alpha)^{-1} \simeq 2$. This implies that $\langle 1/\tau_0 \rangle \simeq 0.5$ GeV. This is quite compatible with the usual notion, based on the old-fashioned perturbation theory, that the inverse of a quantum-transition time should be of the order of the mass of the quanta (i.e., mesonic clusters for the present case) emitted.

With $y_c \sim y_1$, the EPS sheet or the EPS flux tube has the rapidity range $\sim[y_c, Y]$, and essentially does not hadronize on its way to the next nucleon. This EPS then serves as the projectile [indicated as a short heavy line in Fig. 3(c)] for the interaction with the next nucleon. Notice that the rapidity spread of this EPS is large and actually overlaps with that of the next nucleon. This is why this EPS can have appreciable interaction with the next nucleon without having to wait a long time as nor-

mally expected.[15] Our model assumes that the interaction of the EPS with the next nucleon is also governed by DTU dynamics and so the boundaries of the subsequent sheets are again given by Eq. (3.2).

The sheet corresponding to the ETS has rapidity range $\sim[0, Y-y_c]$. So on the average, part of it (the part in the region $[0,y_c]$) will hadronize, and the rest (the part in the region $[y_c, Y-y_c]$) will remain as an excited hadronic system. In principle, the hadronization products and the leftover excited hadronic system can undergo cascade with succeeding nucleons. However, the hadronization products have small energies and the effects of their cascades can safely be neglected. Furthermore, in the energy region of present interest ($50 \leq E_{\text{inc}} \leq 200$ GeV), the energy of the leftover excited hadronic system is also relatively small. Therefore, to the first approximation, its cascades can also be neglected. This then leads to the result of $R_A \cong (1+\bar{\nu}_p)/2$ in agreement with experimental feature (a). A more quantitative estimate on the corrections due to the cascades is presented in the Appendix.[16]

To illustrate the type of differential multiplicity distribution that results from this model, let us consider the simplified version of a plateau for the contribution from each sheet (a more realistic version will be discussed shortly). The two-sheet spectra for pp collision are shown in Fig. 4(a), where I labels the ETS sheet with a plateau $\sim[0, Y-y_c]$ and II the EPS sheet with the plateau $\sim[y_c, Y]$. For $\bar{\nu} > 1$, its suffices to discuss the case of $\bar{\nu}=2$. As indicated in Fig. 3(c), as the result of the interaction with the first nucleon, the ETS gives rise to the plateau I_1, and the second collision gives the ETS plateau I_2 and also the EPS plateau II_2.[18] These distributions together with their sum are shown in Fig. 4(b). This can be easily generalized to other values of $\bar{\nu}$; we see that $(dN/dy)_{hA}$ should be approximately the same as $(dN/dy)_{hp}$ in the large-y region,[19] and $(dN/dy)_{hA} \cong \bar{\nu}(dN/dy)_{hp}$ in the small-y region, in agreement with experimental features (b).

Now we turn to $\bar{p}A$ collisions. Again, first consider $\bar{p}N$ collision. At high energy, the dominant contribution to the Pomeron within the DTU framework is the diagram[20] of Fig. 3(d); cutting this diagram gives Fig. 3(e), which again describes the multiparticle production process a long time after the interaction; shortly after the interaction, the process should be described by Fig. 3(e), but without the extra $q\bar{q}$ pairs. Thus multiparticle production in $\bar{p}N$ collision is described by the evolution of two sheets. One is a short sheet bounded by a quark from the target N and an antiquark from the $\bar{p}$ projectile covering the rapidity range $\sim[y_c, Y-y_c]$. This gives rise to the plateau I in Figs. 3(e) and 4(c). The second is a long sheet bounded by a diquark from N and a antidiquark from $\bar{p}$ covering the rapidity range $\sim[0, Y]$. This gives rise to the plateau $II = II' + II''$ shown in Figs. 3(e) and 4(c). Analogous to the pN case, part of the long sheet hadronizes up to y_c, and the newly created leftover $\bar{q}$ pairs up with the projectile antidiquark $\bar{q}\bar{q}$ to form a new intermediate $\bar{p}$-like antiparticle which serves as the projectile for the interaction with the second nucleon. The short sheet does not hadronize, but similar to the discussion before, in the energy region of the present interest the energy of the short sheet is relatively small and in the first approximation its subsequent cascades can be neglected. Therefore, for $\bar{\nu}=2$, the differential distribution has four contributions. This is illustrated in Figs. 3(f) and 4(d). One is the plateau II_1', from $[0,y_c]$ from the hadronization part of the first long sheet. There are two plateaus I_1 and I_2, from $[y_c, Y-y_c]$ from the two short sheets. And the last one is the plateau $II_2 = II_2' + II_2''$, from $[0, Y]$ from the second long sheet. Upon summing, this gives the same differential distribution and thereby the same R_A as for pA, i.e., $\bar{\nu}$ universality. In other words, if $\bar{\nu}_{pA} = \bar{\nu}_{\bar{p}A}$, then $(dN/dy)_{pA}$

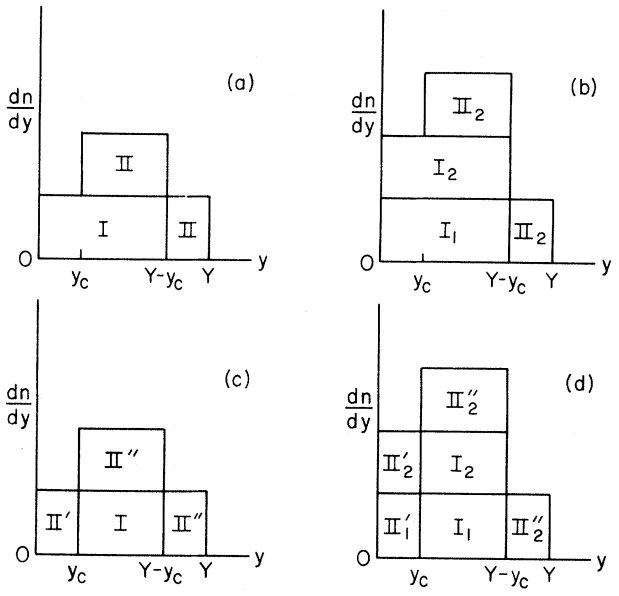

FIG. 4. Rapidity distribution for (a) pN, (b) pA with $\bar{\nu}=2$, (c) $\bar{p}N$, (d) $\bar{p}A$ with $\bar{\nu}=2$.

$=(dN/dy)_{\bar{p}A''}$.

So far we have discussed the $\bar{\nu}$-universality condition for the specific choice of the parameter $y_c \sim y_1$. We now proceed to show that $\bar{\nu}$ universality still holds, as long as the condition $y_c \geq y_1$ is satisfied.

Consider first the pA case. Let us come back to Fig. 3(c). With the difference $\Delta \equiv y_c - y_1 \geq 0$, there will be pair production within the flux tube of the projectile diquark and the target quark, in the range $[y_1, y_1+\Delta]$. On the other hand, for the corresponding $\bar{p}A$ case, the boundary of II_1' will now be extended from y_1 to $y_1+\Delta$. In turn, there will be some additional pair production within the flux tube defined by the diquark and antidiquark pair. So within the plateau approximation, both pA and $\bar{p}A$ cases give rise to the same extra spectra. So, the $\bar{\nu}$ universality is still preserved. For the present case, our model predicts the approximate relation $R \sim (\bar{\nu}+1)/2+(\bar{\nu}-1)\Delta/2(Y-y_1)$. Finally at high energies, since both y_c and y_1 are independent of the laboratory energy of the projectile, the $\bar{\nu}$ universality discussed here is projectile-energy independent, so long as the quantity $\bar{\nu}$ for p and for $\bar{p}$ is kept the same.

Let us now return to the inequality $y_c \geq y_1$. A qualitative estimate based on the color-flux-tube model gives[2(h)] $y_c \cong 1.8$. We recall that the first-moment value $\langle y_1 \rangle \cong 2$. Technically speaking, it is the zero-moment distribution which is relevant in the determination of the effective value of y_1, which, due to the exponential peaking of the y_1 distribution in (3.1), should be substantially less than 2. In other words, we expect the inequality to be satisfied. So far we have only considered the $\bar{\nu}$-universality argument based on the plateau approximation; similar argument should also be valid, at least approximately, for a more realistic spectrum, i.e., a plateau distribution which drops smoothly to zero at both ends. Thus in an approximate sense we have deduced the $\bar{\nu}$ universality at high energies.

Of course, for $\bar{p}N$ interaction there is also an annihilation contribution which is not present for pN interaction. But this annihilation contribution falls off with energy like $s^{-1/2}$, and so at high energy can be neglected compared to the Pomeron contribution.[20,21] In our discussion of hA interactions, we never include this contribution. Nevertheless, we want to point out a verifiable confirmation of a high-lying annihilation contribution. Consider the difference $\Delta \equiv (pp \to px) - (pp \to \bar{p}x)$, where detected inclusive p and $\bar{p}$ are in the central region. The contribution to this difference comes from the baryon annihilation. If the trajectory generated by the annihilation has an intercept $\alpha_A \cong 1/2$,[20,21(a)] then a simple Mueller-Regge analysis says that Δ (at $y_{\mathrm{c.m.}}=0$) $\propto s^{-1/4}$, which is consistent with the data,[22] and Δ should have a $\cosh(y/2)$ dependence. Better data in the future can check these predictions.

Having shown that there is an approximate $\bar{\nu}$ universality for pA and $\bar{p}A$ collisions, we can easily see that this approximate universality also holds for meson-initiated reactions, e.g., πA. A meson-initiated reaction has two types of diagrams. One corresponds to two sheets with comparable rapidity range, as in pA. The second corresponds to a short sheet and a long sheet as in $\bar{p}A$. Since we have already argued that these two diagrams give approximately the same contribution, $\bar{\nu}$ universality follows. Note that if we take the first moment of a quark structure function, a quark in a meson on the average has half the momentum whereas a quark in a baryon on the average has only one-third the momentum. However, what is relevant here, similar to an earlier consideration, is again the zero-moment distribution, so the difference in the quark structure function only manifests itself in the region $x \cong 1$, or $y \cong Y$. Therefore, there is nothing strange about getting approximate $\bar{\nu}$ universality between a meson-initiated and a baryon-initiated reaction.

We now return to pA interactions and discuss the results of our model calculation using a more realistic version of the differential distribution from each sheet. The version we choose is that of Capella *et al.*[6(a)] We emphasize that our results are fairly insensitive to the specific hh model (as long as it agrees with the hh data) used as input.[23] We choose the above model because it is simple, well defined, and above all separates the contribution of the ETS from that of the EPS.

Denote the laboratory rapidity by y, then the model of Ref. 6(a) gives

$$\left[\frac{dN}{dy}\right]_{pp} = f(y - y_{\mathrm{c.m.}} - \Delta) + f(y_{\mathrm{c.m.}} - \Delta - y) , \tag{3.3a}$$

where

$$f(\tilde{y}) = \begin{cases} 1.20(1-\xi)^3, & \tilde{y} \geq 0 \\ \dfrac{0.05+1.15(1-\xi)^2}{1-0.5\xi}, & \tilde{y} < 0 \end{cases} \tag{3.3b}$$

$$\Delta=\tfrac{1}{2}\ln\left[\frac{1+\beta}{1-\beta}\right],\quad \xi=\left|\frac{\mu_T}{\bar{P}}\sinh\tilde{y}\right|, \tag{3.3c}$$

$$\beta=\frac{(2x_0-1)P}{(x_0{}^2P^2+4m_Q{}^2)^{1/2}+[(1-x_0)^2P^2+m_Q{}^2]^{1/2}}. \tag{3.3d}$$

$$\bar{P}=\frac{x_0P-\beta(x_0{}^2P^2+4m_Q{}^2)^{1/2}}{(1-\beta^2)^{1/2}}, \tag{3.3e}$$

where $m_Q=0.33$ GeV was used for the quark mass and $\mu_T=0.33$ GeV for the transverse pion mass. In Eq. (3.3), P is the incident momentum in the c.m., and $Y_{\text{c.m.}}$ is the c.m. rapidity in the laboratory, $\beta(\Delta)$ is the velocity (rapidity) of the EPS's c.m. relative to the overall c.m., and $\bar{P}$ is the momentum of the projectile diquark in the EPS's c.m.. The expression f is related to the quark and diquark fragmentation functions and is determined from e^+e^- data and dimensional counting rules.[24] The first and second terms in (3.3a) correspond, respectively, to the EPS and ETS contributions. Equation (3.3) does not include the forward proton.

It is then straightforward to work out the kinematics of the $(\bar{\nu}-1)$ succeeding inelastic interactions in hA collisions and conclude that the kinematics for the second collision is approximately just that of the first collision except for the substitution $P\to P[x_0(2-x_0)]^{1/2}$. Similar remarks apply for subsequent collisions.

In Fig. 5(a) we show the results of these zero-parameter calculations for $dN/d\eta$ for 200-GeV p-initiated reactions for $\bar{\nu}=2$, 3, 4, as well as the $\bar{\nu}=1$ input. The model calculations are in good agreement with the data,[25] except in the small-η bins where as discussed below we expect the model calculations in the present approximation to underestimate the multiplicity. The results for R_A are shown as the solid line in Fig. 6. Again, the model calculations are approximately equal to (but in the present approximation to be, as expected, slightly less than) the data. Our model calculations for $dN/d\eta$ for 100 and 50 GeV, shown in Figs. 5(b) and 5(c), are also in agreement with the data. Our model prediction for 400-GeV pA interactions is shown in Fig. 5(d).[26] In our model, the energy of each effective projectile is only slightly less than that of its parent; therefore, the elasticity for pA is only slightly smaller than for pp, in agreement with experimental feature (d).

As we said before, on the average, part of the sheet corresponding to the ETS will hadronize, and the rest will remain as a low-energy excited hadronic system which can undergo further cascade with succeeding nucleons. In the Appendix we provide an estimate of the additional multiplicity coming from these cascades. The result with the inclusion of this correction for R_A in 200-GeV pA interactions is shown as the dashed line in Fig. 6. This additional multiplicity is of course in the small-η region, thus accounting for the excess shown in Fig. 5.

Summarizing, we see that this DTU-parton model provides a good and simple explanation of the first five experimental features. The only remaining feature to be explained (which has not yet been calculated in this model) is feature (f), the linear dependence of the dispersion D on $\langle N_{\text{ch}}\rangle$. Since it is known[27] for hh collisions that a two-component model can explain the dispersion data, by including a small diffractive component in the two-sheeted description of multiparticle production, one probably can explain this feature also.

IV. NUCLEUS-NUCLEUS INTERACTIONS

The DTU-parton model can easily be applied to high-energy nucleus-nucleus (AA) interactions.[28] Analogous to the definition (2.1), one defines

$$\bar{\nu}_{A_1/A_2}\equiv\frac{A_1\sigma_{\text{in}}^{NA_2}}{\sigma_{\text{in}}^{A_1A_2}}, \tag{4.1}$$

which can be interpreted to be the average number of inelastically excited nucleons in A_1 in its collision with A_2. Then the DTU-parton model gives

$$R_{A_1A_2}\equiv\frac{\langle N_{\text{ch}}\rangle_{A_1A_2}}{\langle N_{\text{ch}}\rangle_{NN}}\cong\frac{\bar{\nu}_{A_1/A_2}}{2}+\frac{\bar{\nu}_{A_2/A_1}}{2}, \tag{4.2}$$

where the first (second) term is the contribution from the $\bar{\nu}_{A_1/A_2}$ ($\bar{\nu}_{A_2/A_1}$) excited projectile (target) systems in A_1 (A_2). Equation (4.2) reduces to $R_A\cong(1+\bar{\nu}_h)/2$ when A_1 is a nucleon. The rapidity distribution $(dN/dy)_{A_1/A_2}$ is given by superposing the contributions of $\bar{\nu}_{A_1/A_2}$ EPS's and $\bar{\nu}_{A_2/A_1}$ ETS's evaluated at the incident laboratory energy per nucleon. For the model to be realistic, the latter energy must be at least 20–30 GeV per nucleon. Unfortunately, this means that in the foreseeable future the only possible source of data is from cosmic rays.

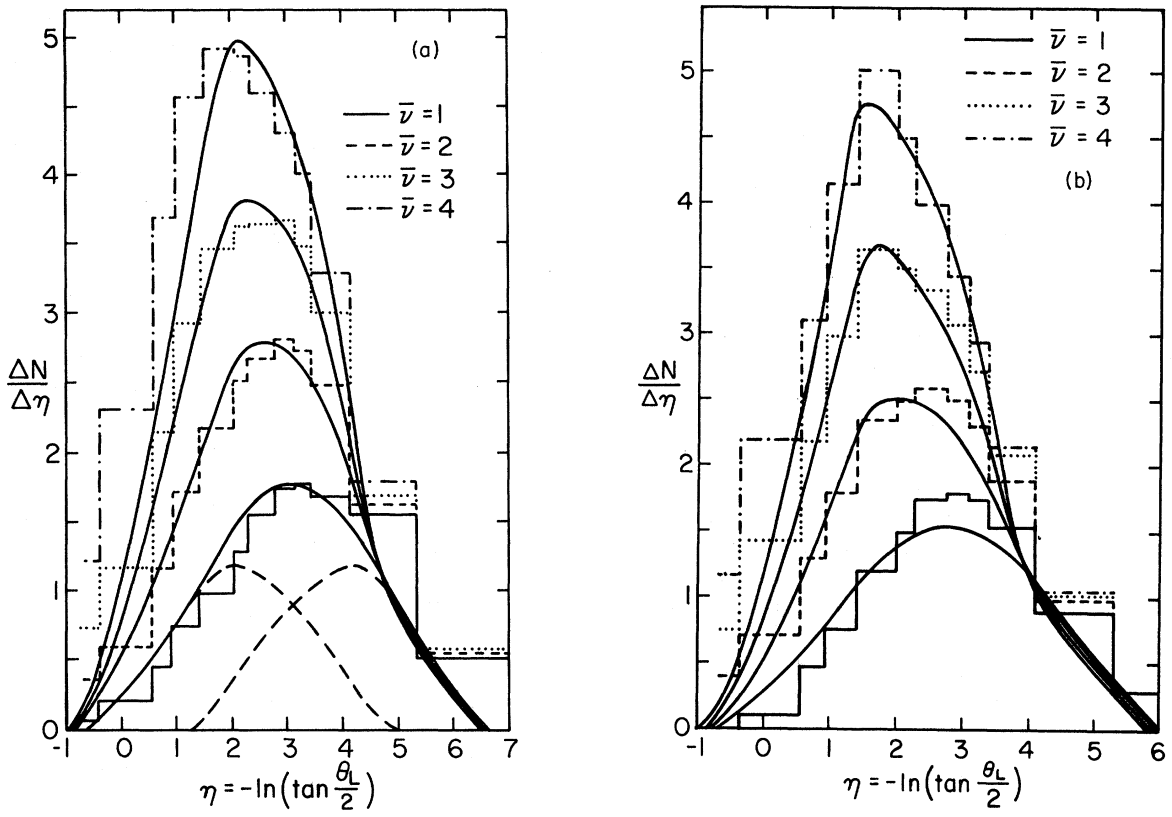

FIG. 5. Laboratory pseudorapidity distributions $dN/d\eta$ for pA collisions. Solid curves are the zero-parameter results of our model; the $\bar{\nu}=1$ curve is the input. (a) At 200 GeV. Also shown are the individual contributions (dashed curves) of the EPS and ETS. The histograms are the data of Ref. 2(d). (b) At 100 GeV. The histograms are the data of Ref. 7(h). (c) At 50 GeV. The histograms are the data of Ref. 7(h). (d) Predictions at 400 GeV.

V. COMPARISON WITH SEVERAL OTHER MODELS

Even though we use the words projectile and target to describe the two excited hadronic systems, the quark-partons from which they are formed are not the same as those of the initial projectile and target. This is especially obvious when considering $\bar{p}A$ interactions. Furthermore, unlike previously proposed two-fireball models[29] which were based on the fragmentation or diffractive model,[30] our DTU two-sheeted model is consistent with short-range correlation. In addition, at asymptotic energies, the two sheets overlap completely in rapidity except for two finite regions at the two ends.

The two-phase model of Fishbane and Trefil[31] assumes that the first collision gives rise to an excited hadronic phase which has a flat distribution over the entire rapidity range and a long deexcitation time, and this excited hadronic phase interacts once more within A. However, the model neglects the interaction of the second (and subsequent) excited hadronic phase formed from the interaction of the first excited hadronic phase. Even ignoring this point, this model's dN/dy is different from our model (even for the same hh input), because in our model the EPS while traversing A does not have much hadronic matter within the rapidity interval defined by its diquark and quark.

The parton model of Brodsky *et al.*,[28] which is also similar to the model of Capella and Kryzwicki,[32] assumes that on the average $\bar{\nu}_h$ wee partons of the projectile interact with the wee partons of the same rapidity in $\bar{\nu}_h$ different nucleons in A, and also assumes that cascading does not occur. It gives at asymptotic energy the result

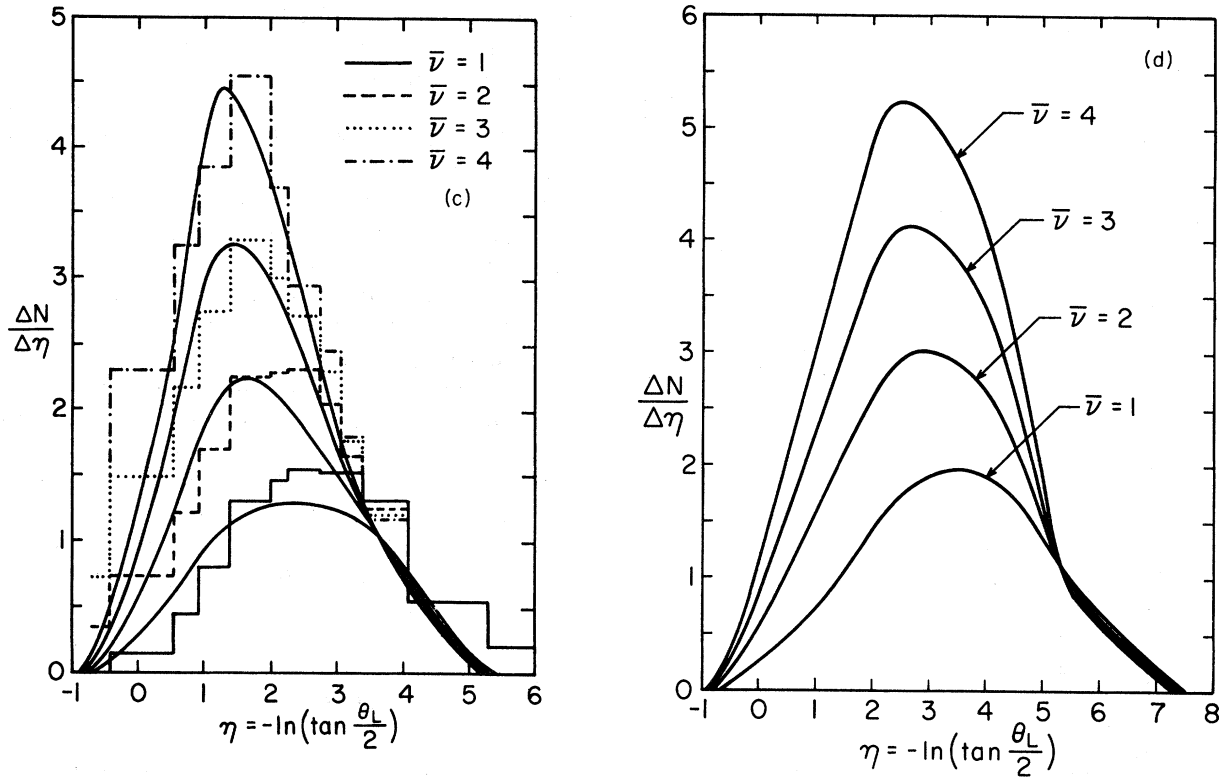

FIG. 5. *(Continued.)*

$R_A = \bar{\nu}_h/(\nu_h+1)+\bar{\nu}_h/2$. In comparison with our model, this parton model corresponds to a one-chain hh process. In addition, this model is applicable only in the central region, and the inclusion of the fragmentation contributions is done by the introduction of a parameter, whereas our model is valid for the whole rapidity range.

Recently, Capella and Tran,[33] also motivated by the DTU-parton approach, proposed a model which is similar although not identical to our model. Their input is an infinitely composite projectile, whose constituents interact with the target nucleons, and the boundaries of the various sheets are given by the quark structure functions. In particular, for pA collision with $\bar{\nu}=2$, the sheet associated with the diquark of the second nucleon is bounded above by an energetic $(x>0)$ q from the sea of the incident p. From our point of view, even though the incident hadron is also composite (i.e., it contains valence quarks and virtual $q\bar{q}$ pairs or gluons), the pulling apart of the virtual $q\bar{q}$ pair is the consequence of the flux-tube mechanism, which requires a characteristic proper time τ_0. Therefore, an energetic (with $y>y_c$) virtual $q\bar{q}$ pair does not have time to materialize and then to interact with the succeeding nucleons. We believe this point of view is more in the spirit of the DTU description of the soft physics. In detail, the sheet number three for the pA case with $\bar{\nu}=2$, which they have illustrated in their Fig. 1, can only be partially present in our model. More specifically, when $y_c>y_1$, this "sheet" for us would be the extra spectrum ranging from y_1 to a constant upper limit y_c, while the corresponding upper limit in their model grows with energy. At present energies this results in a negligible phenomenological difference. But at asymptotic energies, ignoring the secondary cascades, they predict $R\sim\bar{\nu}$, and we have $R\sim(\bar{\nu}+1)/2$. Furthermore, contrary to their claim, our model does have the $\bar{\nu}$-universality feature,[3(b)] as stated earlier in Ref. 3(a).

Our present model suppresses a large excess multiplicity by assuming that there is not enough time to produce the energetic secondaries. This is in contrast with our earlier model.[34] There we assumed that even though energetic secondaries are produced, for them to substantially interact with the succeeding nucleons, they must generate a multiperipheral chain containing small-rapidity partons, and to do this takes a long time. We called

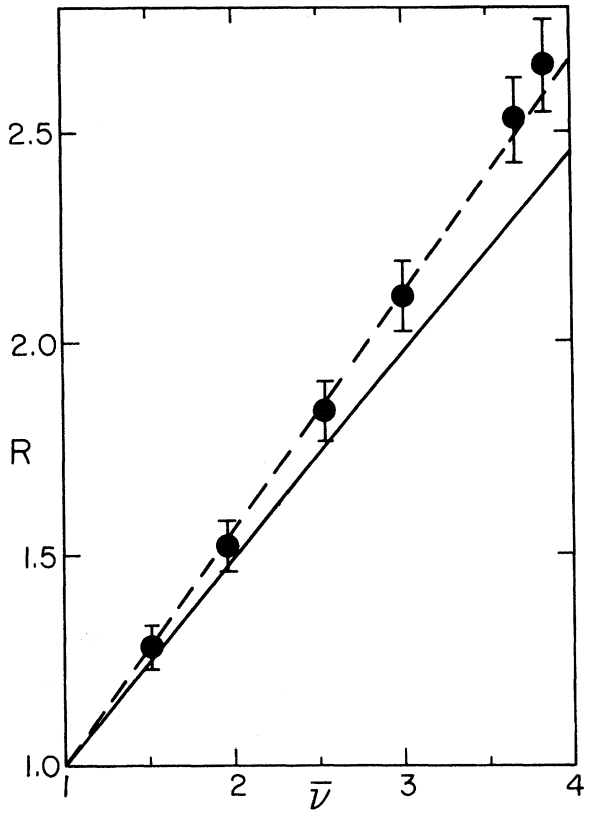

FIG. 6. The multiplicity ratio R_A versus $\bar{\nu}_p$ for 200-GeV pA collisions. Data are from Ref. 2(d). The dashed line and solid line are the results of our model with and without including further interactions of the ETS's as explained in the text and in the Appendix.

this latter process the maturing process. We recall that the immaturity concept was already discussed by Feinberg[35(a)] more than a decade ago following a much earlier suggestion of Landau and Pomeranchuk.[35(b)] Feinberg's model has recently been given a more general formulation where the immaturity effect is referred to as the Zeno effect.[36] For example,[37] Fig. 7 illustrates the suppression factor due to the Zeno effect $Q(y,Y)$ [see Eq. (35) of Ref. 36(a)], for the production of a secondary particle of rapidity y from a primary particle of rapidity $Y=5$. The curve corresponds to the following picture: The higher the secondary rapidity, the more quickly it is produced, and, in turn, the less the suppression factor. In our model of Ref. 34 mentioned above, one considers a different picture. There the suppression factor was parametrized by $Q(y)=\eta Q'(y_c,Y)$, where Q' is similar to $Q(y,Y)$, except Q' is somewhat simpler in form, and η is the induced maturity factor. The quantity $Q(Y)$ of Ref. 34 is also shown in Fig. 7 for comparison. We see that in the moderate and the large rapidity region (e.g., $y \gtrsim 2.5$), the numerical effect of the two curves turned out to be similar. One may say that the Zeno effect here partially restores the production of the large-rapidity secondaries and it mimics the induced maturity effect proposed earlier. One may also regard Ref. 36 as a theoretical motivation for the phenomenological parametrization of the induced maturity effect, at least in a certain rapidity region.

One may question whether the immaturity concept is consistent with the Glauber theory[38] for calculating σ_{in}^{hA}, which never mentioned any immaturity. This question is unwarranted because σ_{in}^{hA} can always be expressed in a form which does not contain any immaturity factor.[39] This can also be seen explicitly by writing out the multiple-scattering series and noticing that the individual terms may contain the immaturity factor, but the sum does not.

VI. CONCLUSION

The purposes of discussing high-energy hA interactions are to learn about the space-time development of hh interactions and to differentiate various hh multiparticle production models. From the experimental data [especially features (a) and (b) presented in Sec. II and the theoretical discussion of Secs. III and V], one concludes that to avoid excessive cascading there must be a long time scale involved in hh interactions. In the models of Refs. 15 and 17, this is the time it takes a high-energy hadron to generate a multiperipheral

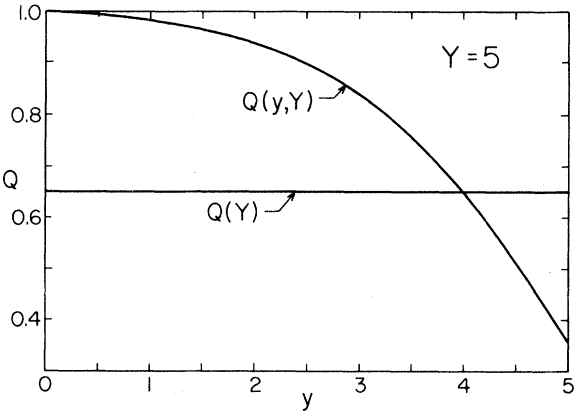

FIG. 7. A comparison of the immaturity factor $Q(y,Y)$ and $Q(Y)$ of Refs. 36 and 17, respectively, at $Y=5$.

chain containing small-rapidity partons so that it can have appreciable interaction with an at-rest hadron. Or saying it in another way, this is the time it takes high-energy bare particle to dress up to be a physical hadron and so to have an appreciable inelastic cross section upon collision with another hadron. In the present DTU two-sheeted model, this is the time it takes the energetic sheet to evolve into its asymptotic multihadron state. This long time scale rules out any sort of instantaneous production model such as the naive cascade model.[40]

Some of the successful hA models also tie in with recent developments for models of hh interaction. For example, the models of Refs. 28, 32, and 41 rely heavily on parton-model ideas, and the present model as well as that of Ref. 33 is partially based on the two-sheeted description of the Pomeron and soft multiparticle production within the dual-topological-unitarization approach, and partially based on the colored-quark-parton model and color confinement. All of this leads one to speculate that one can also see glimpses of the true underlying theory governing strong interactions by looking at hA interaction.

We also remark that there may be other interesting effects, besides the ones discussed here, which arise from interactions involving nuclear targets. One is the A dependence for the inclusive cross section for large-p_T secondaries. The data[42] show that this A dependence for a π secondary can be parametrized as $A^{\alpha(P_T)}$, where $\alpha(P_T)\cong 0.9$ for $P_T \leq 1$ GeV/c and increases to $\alpha(P_T)\cong 1.1$ for $P_T \geq 4$ GeV/c. This A dependence is most likely due to multiple scattering[43] inside the nucleus. Another effect is the importance of the two-step process $p+A\to\pi+A'+\cdots\to\mu^+\mu^-+\cdots$ as compared to the one-step process $p+A\to\mu^+\mu^-+\cdots$. Since the π has a valence antiquark, the two-step process may be significant if the production process is dominated by the Drell-Yan mechanism.[44] Another interesting effect is that hA interaction may provide a laboratory to "see" quark-hadron scattering, because for a large-p_T process, one of the incident quarks may be given a large p_T and so be separated in momentum space from its partners; it then interacts with another nucleon in the nucleus.

In all the successful hA models, there must be a mechanism to suppress certain degrees of freedom so as to suppress the multiplicity. This mechanism may take the form of bare particles which have small inelastic-collision probability until a sufficiently long time has elapsed, or it may take the form of the absence of energetic secondaries until a long time has elapsed. Whatever the mechanism, it seems that the hh multiparticle production process at short times is different from the asymptotic description that one obtains from ordinary hh scattering experiments. To reach the short times discussed here, we need matter of nuclear density or higher. This leads, therefore, to the extremely relevant question of whether the lessons that we have learned from high-energy hA interactions have any astrophysical implications, as in neutron stars, black holes, or the early universe. Investigations in this direction are underway. Some ramifications already appear to be very interesting.[36]

During the past decade, great progress, both experimental and theoretical, has been made in the field of hA interactions. We can look forward to some more exciting progress during this decade.

ACKNOWLEDGMENTS

This work was supported in part by the U. S. Department of Energy. We thank W. -q. Chao for useful discussion and correspondence and for collaboration in the initial stage of this work.

APPENDIX

In this appendix we provide a rough estimate for pA collision of the additional multiplicity due to the further interactions of the ETS with the succeeding nucleons in A. In the text we said that, on the average, part of the ETS sheet hadronizes and the rest does not. Here we consider the simplified but approximately equivalent problem of assigning a probability Q that the ETS does not evolve into its asymptotic multihadron state upon reaching the succeeding nucleon N. We parametrize this probability Q by $e^{-t/\gamma\tau_0}\cong e^{-2/\gamma}$, where we set $\tau_0\cong 1/2m_\pi$, and $t\cong 1/m_\pi$ to be the time to travel the average internucleon distance, and γ is the time-dilation factor.[45] Now, let P be the probability that an EPS or ETS would undergo an inelastic collision in a collision with N.[46] Then the probability P' that an EPS or ETS does not evolve into its final state after traveling the average internucleon distance and then does undergo an inelastic collision with the subsequent N is given by $P'_{\rm EPS}\cong P$ or $P'_{\rm ETS}\cong Pe^{-2/\gamma_{\rm ETS}}$.

It suffices to include only those interactions of the ETS's with those succeeding N's which had not

interacted inelastically with the EPS (we call these unwounded nucleons), because the excitation of N amounts to the formation of a sheet and this provides a natural saturation mechanism for its excitation.[47] We want to derive a formula for the probability p_i that the unwounded ith nucleon experiences an inelastic collision with the preceding ETS's. It is obvious that p_2 is given by

$$p_2 \cong P(1-P)P'_{\rm ETS} , \tag{A1}$$

where the first factor is the probability that the incident proton undergoes an inelastic collision with the first N to produce an ETS, the second factor is the probability that the EPS leaves the second N unwounded, and the third factor is the probability that the ETS does not evolve into its multihadron final state and then does undergo an inelastic collision with the second N. Similarly, p_3 is given by

$$p_3 \cong [2P(1-P)](1-P)P'_{\rm ETS} + P^2(1-P)[1-(1-P'_{\rm ETS})^2] , \tag{A2}$$

where the first (second) term is the contribution when there is one (two) ETS. The general formula is then

$$p_m \cong \sum_{i=1}^{m-1} \phi_i^{m-1}(1-P)[1-(1-P'_{\rm ETS})^i] , \tag{A3}$$

where

$$\phi_i^l = \frac{l!}{i!(l-i)!} P^i (1-P)^{l-i} . \tag{A4}$$

The multiplicity from each such collision is to be evaluated at the laboratory energy of the ETS.[48] Also, only one-half of this is an additional multiplicity (as the contribution from the first-generation ETS's is already included). The ratio r of this charged multiplicity to $\langle N_{\rm ch} \rangle_{pN}$ (the latter evaluated at the incident energy) is approximately $r \cong 0.27$.[49] Therefore, the additional contribution ΔR_A to R_A for a nucleus of $\bar{k}$ nucleons in length is[50]

$$\Delta R_A \cong r \sum_{i=2}^{\bar{k}} p_i . \tag{A5}$$

---

*Present address.

[1]Macroscopic distance here means any distance which is much larger than the typical range of strong interaction, i.e., 1 fm.

[2]For previous reviews, see (a) K. Gottfried, in *High Energy Physics and Nuclear Structure—1973,* proceedings of the Fifth International Conference, Uppsala, Sweden, edited by G. Tibell (North-Holland, Amsterdam/American Elsevier, New York, 1974); (b) W. Busza, in *High Energy Physics and Nuclear Structure—1975,* proceedings of the Sixth International Conference, Santa Fe and Los Alamos, edited by D. E. Nagle *et al.* (AIP, New York, 1975); (c) L. Bertocchi, *ibid;* (d) W. Busza *et al.*, in *Proceedings of the XVIII International Conference on High Energy Physics, Tbilisi, 1976,* edited by N. N. Bogolubov *et al.* (JINR, Dubna, 1977); (e) N. N. Nikolaev, in *Multiparticle Production on Nuclei at Very High Energies,* proceedings of the Trieste Topical Meeting, 1976, edited by G. Bellini, L. Bertocchi, and P. G. Ranciota (International Centre for Theoretical Physics, Trieste, 1976); (f) A. Bialas, in *Proceedings of the First Workshop on Ultra-Relativistic Nuclear Collisions, Berkeley, California, 1979* (LBL, Berkeley, 1979); (g) D. M. Tow, in *Proceedings of the 1980 Guangzhou Conference on Theoretical Particle Physics, Guangzhou, China* (Science Press, Beijing, and Van Nostrand Reinhold, New York, 1980); (h) C. B. Chiu, in *High Energy Physics—1980,* Proceedings of the XX International Conference, Madison, Wisconsin, edited by L. Durand and L. G. Pondrom (AIP, New York, 1981).

[3]For abbreviated discussion of portions of this model, see (a) W. -q. Chao, C. B. Chiu, Z. He, and D. M. Tow, Phys. Rev. Lett. 44, 518 (1980); (b) C. B. Chiu and D. M. Tow, Phys. Lett. 97B, 443 (1980).

[4](a) H. Lee, Phys. Rev. Lett. 30, 719 (1973); (b) G. Veneziano, Phys. Lett. 43B, 413 (1973); 52B, 220 (1974); Nucl. Phys. B74, 365 (1974); (c) H. -M. Chan, J. E. Paton, and S. T. Tsou, *ibid.* B86, 479 (1975); H.-M. Chan, J. E. Paton, S. T. Tsou, and S. W. Ng, *ibid.* B92, 13 (1975); (d) For a review see, e.g., G. F. Chew and C. Rosenzweig, Phys. Rep. 41C, 263 (1978); (e) For a discussion of the similarity between the DTU Pomeron and the dual-resonance-model Pomeron, see C. B. Chiu and S. Matsuda, Nucl. Phys. B134, 463 (1978); P. Aurenche and L. Gonzalez Mestres, Phys. Rev. D 18, 2995 (1978).

[5]G. Cohen-Tannoudji *et al.*, Phys. Rev. D 19, 3397 (1979); G. Cohen-Tannoudji *et al.*, *ibid.* 21, 2699 (1980); and earlier references therein.

[6](a) A. Capella *et al.*, Phys. Lett. 81B, 68 (1979); (b) A. Capella *et al.*, Z. Phys. C 3, 329 (1980).

[7](a) W. Busza *et al.*, Phys. Rev. Lett. 34, 836 (1975); (b) see Ref. 2(d); (c) J. R. Florian *et al.*, Phys. Rev. D 13, 558 (1976); (d) C. Halliwell *et al.*, Phys. Rev. Lett. 39, 1499 (1977); (e) D. Chaney *et al.*, *ibid.* 40, 71 (1978); (f) J. E. Elias *et al.*, *ibid.* 41, 285 (1978); (g) D. Chaney *et al.*, Phys. Rev. D 19, 3210 (1979); (h) J. E. Elias *et al.*, *ibid.* 22, 13 (1980).

[8]See, e.g., Appendix A of Ref. 2(g).

[9]The constant b (a) is slightly larger (smaller) than $\frac{1}{2}$.

[10]See, e.g., Ref. 7(g).

[11]A. Casher, J. Kogut, and L. Susskind, Phys. Rev. D 10, 732 (1974); A. Casher, H. Neuberger, and S. Nussinov, *ibid.* 20, 179 (1979).

[12]E. Brezin and C. Itzykson, Phys. Rev. D 2, 1191 (1970); C. B. Chiu and S. Nussinov, *ibid.* 20, 945 (1979).

[13]C. B. Chiu, in *High Energy Hadronic Interactions,* proceedings of the XIV Recontre de Moriond, Les Arcs, France, 1979, edited by J. Trân Thanh Vân (Editions Frontieres, Gif-sur-Yvette, 1979).

[14]C. B. Chiu and S. Matsuda, Nucl. Phys. B134, 463 (1978); P. Aurenche and L. Gonzalez Mestres, Phys. Rev. D 18, 2995 (1978).

[15]See, e.g., J. Koplik and A. H. Mueller, Phys. Rev. D 12, 3638 (1975).

[16]In the Appendix we provide a rough estimate of the correction due to these cascades. Even at asymptotic energies, it would lead to a result that R_A is between $(1+\bar{\nu}_p)/2$) and $(1+\bar{K}/2)$, where $\bar{K}$ is the geometric average number of nucleons that the incident hadron h sees in the nucleus (Ref. 17). Since $\bar{K}\cong 1.3\bar{\nu}_P \cong 1.6\bar{\nu}_\pi$, the correction is not very large when $h=p$, but is larger when $h=\pi$.

[17]G. Bialkowski, C. B. Chiu, and D. M. Tow, Phys. Lett. 68B, 451 (1977); Phys. Rev. D 17, 862 (1978).

[18]Here we neglect the small decrease in the incident energy of the second projectile as compared to the original incident energy. This neglect was shown in Ref. 3(a) to be a very good approximation.

[19]Since the EPS has a slightly smaller energy than its present, $(dN/dy)_{hA}$ is slightly smaller than $(dN/dy)_{hp}$ for $y\sim y_{\max}$, in agreement with experimental feature (e).

[20]Y. Eylon and H. Harari, Nucl. Phys. B80, 349 (1974). See also, G. C. Rossi and G. Veneziano, *ibid.* B123, 507 (1977).

[21](a) B. R. Webber, Nucl. Phys. B117, 445 (1976); (b) H. -M. Chan and S. T. Tsou, *ibid.* B118, 413 (1977).

[22]B. Alper *et al.*, Nucl. Phys. B100, 237 (1975).

[23]For example, the more refined version of Ref. 6(b) gives essentially the same results. We also got similar results using a two-temperature thermodynamic model; this model is similar but not identical to that of T. F. Hoang, Phys. Rev. D 12, 296 (1975).

[24]In Eq. (3.3) we use 0.92 for x_0 and 1.20 for the normalization of f at $\xi=0$, instead of the respective numbers of 0.95 and 1.35 of Ref. 6(a). There are two reasons for this small change. Ours gives better agreement with the pp data of Busza *et al.*, which is the input for our model's pA calculations. Second, a smaller x_0 gives a smaller rise over the energy range $\sqrt{s}\cong 20-60$ GeV for the central height of pp collisions, consistent with our belief that at least part of this rise is due to the threshold production of $N\bar{N}$ clusters [C. -I. Tan and D. M. Tow, Phys. Rev. D 9, 2176 (1974); C. B. Chiu and D. M. Tow, *ibid.* 15, 3313 (1977)]. We have checked that our parametrization is equally consistent with the e^+e^- data from which it was determined [Ref. 6(a)]. The peaking of the diquark x at $x_0\cong 1$ is due to the peaking of the valence-quark structure function near $(1-x)\cong 0$. In DTU language, $x\cong 1$ (or 0) corresponds to ordinary Reggeon (or exotic-meson) exchange [Refs. 4, 6(b), and 14].

[25]Recall that we are considering only inelastic events and that the forward-proton contribution has not been included in our $\bar{\nu}=1$ input. This is the reason for the excess near $\eta\sim 5$.

[26]There is one set of experimental data at 400 GeV [F. Fumuro, R. Ihara, and T. Ogata, Nucl. Phys. B152, 376 (1979)]. However, their normalization seems to be very different from those at several lower energies (50–300 GeV) (Ref. 7).

[27](a) L. Van Hove, Phys. Lett. 43B, 65 (1973); (b) K. Fialkowski and H. I. Meittinen, *ibid.* 43B, 493 (1973); (c) C. B. Chiu and K. -H. Wang, Phys. Rev. D 8, 2929 (1973).

[28]See also the discussion of S. J. Brodsky, J. F. Gunion, and J. H. Kühn, Phys. Rev. Lett. 39, 1120 (1970).

[29]A. Dar and J. Vary, Phys. Rev. D 6, 2412 (1972); P. M. Fishbane and J. J. Trefil, *ibid.* 9, 168 (1974).

[30](a) C. Quigg, J. -M. Wang, and C. N. Yang, Phys. Rev. Lett. 28, 1290 (1972); (b) R. Hwa, *ibid.* 26, 1143 (1971); (c) M. Jacob and R. Slansky, Phys. Rev. D 5, 1847 (1972).

[31]P. M. Fishbane and J. S. Trefil, Phys. Lett. 51B, 139 (1974).

[32]A. Capella and A. Kryzwicki, Phys. Lett. 67B, 84 (1977); Phys. Rev. D 18, 3357 (1978).

[33]A. Capella and J. Trân Thanh Vân, Phys. Lett. 93B, 146 (1980).

[34]Ref. 17; see also M. Hossain and D. M. Tow, Phys. Rev. D 21, 1842 (1980).

[35](a) E. L. Feinberg, Zh. Eksp. Teor. Fiz. 50, 202 (1966) [Sov. Phys.—JETP 23, 132 (1966)]; (b) L. D. Landau and I. Ya. Pomeranchuk, Dok. Akad. Nauk SSSR 92, 535 (1953); 92, 735 (1953).

[36](a) P. Valanju, E. C. G. Sudarshan, and C. B. Chiu, Phys. Rev. D 21, 1304 (1980); (b) P. Valanju, Ph.D. dissertation, University of Texas at Austin, 1980 (unpublished).

[37]Private communication from P. Valanju. We thank Dr. Valanju for discussions on the comparison between $Q(y,Y)$ and $Q(Y)$ given here.

[38]See, e.g., R. J. Glauber, in *High Energy Physics and Nuclear Structure,* edited by G. Alexander (North-Holland, Amsterdam, 1967).

[39]See Eq. (2.1) and footnote 10 of Ref. 34.

[40]P. M. Fishbane and J. S. Trefil, Phys. Rev. D 3, 231 (1971); A. Dar and J. Vary, *ibid.* 6, 2412 (1972).

[41]N. N. Nikolaev, in *Multiparticle Production on Nuclei at Very High Energies,* proceedings of the Trieste Topical Meeting, 1976, edited by G. Bellini, L. Bertocchi,

and P. G. Ranciota (International Centre for Theoretical Physics, Trieste, 1976).
[42]J. W. Cronin *et al.*, Phys. Rev. D 11, 3105 (1975); L. Kluberg *et al.*, Phys. Rev. Lett. 38, 670 (1977).
[43]J. H. Kühn, Phys. Rev. D 13, 2948 (1976).
[44]S. D. Drell and T. M. Yan, Phys. Rev. Lett. 25, 316 (1970); Ann. Phys. (N. Y.) 66, 578 (1971).
[45]For an incident energy of 200 GeV, $\gamma_{\rm EPS}$ and $\gamma_{\rm ETS}$ are, respectively, 34 and 3. Therefore, this probability Q for the EPS can be set approximately equal to one.
[46]In the numerical calculation we assume that the EPS or ETS has the same P as that of a proton which was estimated in Ref. 17 to be 0.64.
[47]Another argument to support this assertion is that two ETS's have small relative momentum and so even upon a collision very little additional multiplicity will result.
[48]This energy is $\sim$17 GeV when the incident energy is 200 GeV.
[49]See, e.g., D. M. Tow, Phys. Rev. D 7, 3535 (1973).
[50]One can show that $\bar{k}$ is related to $\bar{v}$ by $\bar{v}=\bar{k}P$ [see Appendix A of Ref. 2(g)].